Proceedings of the 6th European VLBI Network Symposium
Ros, E., Porcas, R.W., Lobanov, A.P., & Zensus, J.A. (eds.)
June 25th-28th 2002, Bonn, Germany

Observations the OH Megamaser galaxies Arp 220 and IRAS 10039−3338

E. Rovilos[1], P. J. Diamond[1], C. J. Lonsdale[2] C. J. Lonsdale[3], and H. E. Smith[4]

[1] Jodrell Bank Observatory, University of Manchester, Macclesfield, Cheshire, SK11 9DL, UK
[2] MIT Haystack Observatory, Off Route 40, Westford, MA 01886, US
[3] Infrared Processing and Ananysis Center, California Institute of Technology, 100-22, Pasadena, CA 91125, US
[4] Center for Astrophysics and Space Sciences, University of California, San Diego, La Jolla, CA 91125, US

Abstract. MERLIN observation of the OH Megamaser galaxy Arp 220 as well as VLBA observations of IRAS 10039-3338 are presented. The continuum emission of Arp 220 does not seem to coincide with the maser for the western component. IRAS 10039-3338 shows a peculiar structure, especially in its velocity field, possibly due to a multiple nucleus structure.

1. Introduction

Ultra Luminous Infrared Galaxies are so called because their infrared luminosity is greater than the luminosity in all other wavelengths combined. The reason for that is the existence of enormous amounts of hot dust grains in their central regions, which absorb optical and other wavelength radiation and re-emit it in the infrared. The mechanism that heats the grains is a starburst, although in many cases, especially when the infrared luminosity is very high ($> 10^{12}L_{\odot}$), active galactic and Seyfert-like nuclei start playing an important role. A detailed overview of the properties of these galaxies can be found in Sanders and Mirabel, 1996.

One of the most striking properties of these galaxies is that they tend to host very powerful OH masers, so called Megamasers. They were first discovered in Arp 220 by Baan et al. in 1982 and are the most powerful OH masers observed. They were first thought to be unsaturated, coming from molecular regions with a physical extent of several hundred parsecs (Baan, 1985) but higher resolution imaging revealed a much more compact structure (Diamond et al. 1989, Lonsdale et al. 1998 for Arp 220, Diamond et al. 1999 for III Zw35 and IRAS 17028-0014). The compact components seem to consist only of the 1667 MHz line, whereas there are also diffuse components covering the overall region, consisting of both the 1667 and the 1665 MHz lines.

The properties of the galaxies that host OH Megamasers are also very interesting. Recently, Philström et al. (2001) observed a disk-like structure in III Zw35, similar to that found in Mrk 273 by Yates et al. 2000. Such a structure might explain the broad spectral lines observed in OH Megamasers. Arp 220 also appears to be a rotating disk, as seen in HI absorption (Mundell et al. 2001) and CO emission (Sakamoto et al. 1999). The existence of radio supernovae in the nuclear regions of Arp 220 (Smith et al. 1998) and possibly in Mrk 273 (Carilli et al. 2000) demonstrate that the starburst is the main power source of those galaxies, although the co-existence of another power source is always possible.

In this paper we present MERLIN observations of Arp 220 where the saturated nature of the maser emission of the western nuclear region is demonstrated, and we also show recent VLBA observations of the OH Megamaser of IRAS 10039-3338. This source was discovered in 1988 by Kazès et al. using the Nancay telescope.

2. Observations and data reduction

2.1. Arp 220

The data were taken on 13 April 1998 by seven MERLIN antennas including the 76 m Lovell telescope, observing only with left-hand circular polarization. The observations covered a total bandwidth of 4 MHz divided into 256 channels, the central channel being set at a frequency of 1666.38 MHz. The initial editing and gain elevation corrections as well as preliminary flux calibration were made using local MERLIN software and then 'AIPS' and 'difmap' were used for further calibration, imaging and continuum subtraction. This resulted in a continuum image and a 121-channel wide cube.

2.2. IRAS 10039-3338

The data were taken on 12 October 1998 by 11 VLBA antennas including the phased VLA, observing with dual circular polarization. The observations covered a total bandwidth of 8 MHz divided into 512 spectral channels, observing at frequency of 1607.27 MHz. The calibration was made using standard VLBA procedures with 'AIPS' and resulted in a 151-channel wide cube.

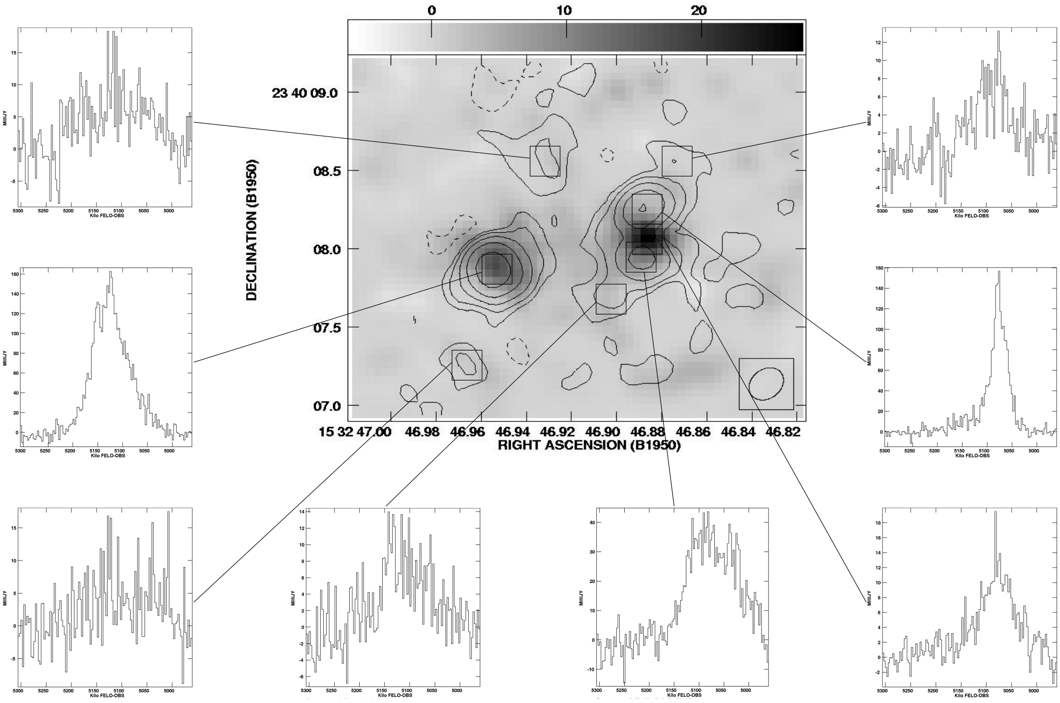

Fig. 1. The continuum and spectral line emission of Arp 220. The greyscale map represents the continuum and the contours the maser emission. To make the line map we summed all the velocities (4961.7 - 5304.6 Km/sec of the naturally weighted images. The contours represent (-4), 4, 8, 16, 32 and 64 % of the peak flux density, which is 3.033 Jy/beam.

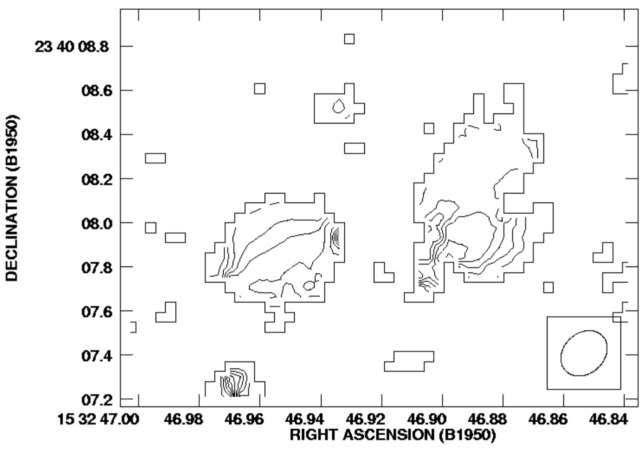

Fig. 2. The velocity map of Arp 220. The contours represent velocities from 5030 to 5200 Km/sec every 10 Km/sec. Only data whose integrated flux density is greater than 15 mJy/beam are selected.

3. Discussion

3.1. Arp 220

The continuum (in greyscale) as well as the spectral line map (in contours) are shown in figure 1. The two components of the continuum emission are separated by 1 arcsec and are at the same positions as the 1.3 mm (Sakamoto et al. 1999) and the 4.83 GHz (Baan and Haschick, 1985) continuum peaks. The flux densities are 97±9 and 109±10 mJy for the eastern and western region respectively. We should note here that the limits of these regions are not well defined because of the overall diffuse emission, so these numbers are lower limits. The flux density of the overall region is 260 ± 50 mJy, close to the 1.4 GHz overall continuum emission derived by Mundell et al. 2001 (285.4 ± 14.3 mJy).

As we can see in Figure 1, in the eastern nuclear region the position of the masers seems to coincide with that of the continuum, in agreement with the model suggesting a screen of molecular material amplifying the continuum emission (Baan, 1985). On VLBI scales (Lonsdale et al. 1998) the 1667 MHz maser emission is clumped in small parsec-scaled regions with distinct velocities, something that can explain the very broad spectrum of that region (spectrum 2 in Figure 1), if we assume that all the regions with different velocities are blended together in MERLIN scales.

In the western region, all the 1.6 GHz (this paper), the 1.4 GHz (Mundell et al. 2001) the 4.8 GHz (Baan et al. 1995) and the 1.3 mm (Sakamoto et al. 1999) continuum emission seem to come from the same area as the CO emission and HI absorption. The supernovae (Smith et al. 1998) are situated there, close to its northern border, possibly providing energy to heat the dust grains and thus generate infrared and radio continuum emission. The position of the OH maser emission is however different, as it arises from regions north and south from the continuum. Mundell et al. (2001) assumes that the northwestern maser emission peak coincides with the continuum, we are however confident that this is not the case, as we extracted

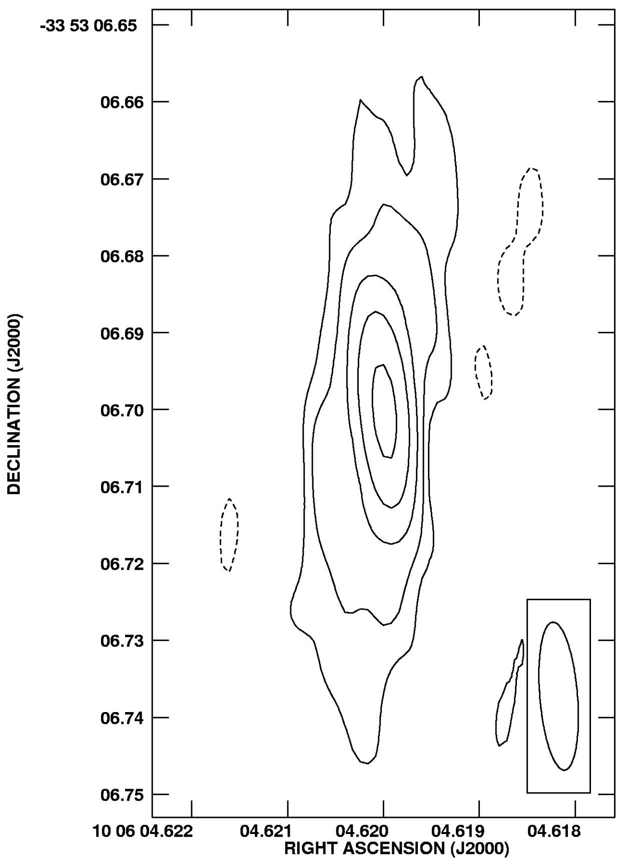

Fig. 3. The spectral line emission of IRAS 10039-3339. All channel maps were summed and the contours represent (-5), 5, 10, 20, 40 and 80 % of the peak flux density, which is 3.135 Jy/beam.

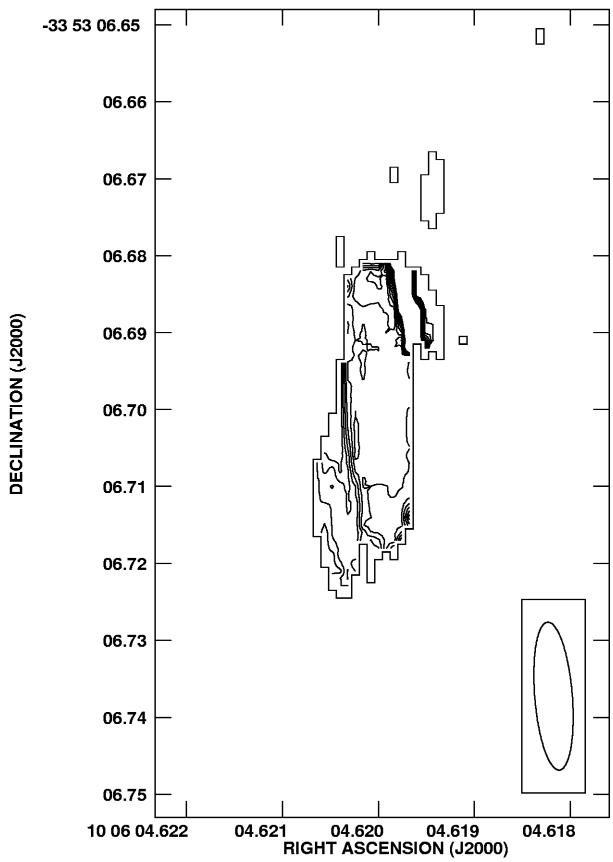

Fig. 4. The velocity map of IRAS 10039-3339. The contours represent velocities from 10070 to 10120 Km/sec every 5 Km/sec. Only data which flux density is greater than 15 mJy/beam are selected.

both the continuum and spectral line maps of Figure 1 from the same dataset performing the same self calibration. This suggests that the OH emission is saturated; the lower limit for the amplification factor is 260 ± 5 and 93 ± 5 for the northwestern and the southwestern region respectively.

Figure 2 shows the moment map of Arp 220. There is a clear velocity gradient of $(370 \pm 40) km sec^{-1} kpc^{-2}$ in the eastern region. Mundell et al. 2001 find $(1010 \pm 20) km sec^{-1} kpc^{-2}$ for the HI. If we assume that the OH arises from a circular rotating disk, its radius is $(79 \pm 5) pc$ and its dynamical mass is $(16 \pm 5) \times 10^6 M_{\odot}$. This is smaller by a factor of 70 than the mass calculated from HI absorption. This difference can be explained if the OH gas lies in the inner part of the molecular disk compared to the HI and that it rotates as a solid body rather than having a keplerian motion.

3.2. IRAS 10039-3338

We can see the integrated spectral line image (1667 MHz only) of IRAS 10039-3339 in Figure 3. The peak flux density detected (derived from Gaussian fitting of the emission of the brightest channel) is $(174\pm6) mJy$, about 67% of the single dish peak flux density (Killeen et al. 1996). The beam is shown on the bottom right of the image and is 19.29×4.89 mas, which is 13.1×3.3 pc, if we assume a distance of 140 Mpc. This means that the maser emission comes from a region well within the nucleus of the galaxy. The size of IRAS 10039-3338 is 32×22 kpc (Kazès et al. 1990). Figure 4 shows the velocity map of this galaxy, where we can clearly see that there are distinct components present with different velocities. The velocity differences are $\sim$ 13 km/sec for the northeastern component (blueshifted) and $\sim$ 80 km/sec for the northwestern (redshifted).

The spectrum of the galaxy can be seen in Figure 5a. This spectrum has been taken from the whole region, and we can clearly detect an underlying 100 km/sec wide component, as well as multiple narrow components, as in Kazès et al. 1990. If we however take the spectrum of a small region of the galaxy, just at the center of the central emission bulk, we do not detect the wide underlying component, but do detect the narrow components (Figure 5b). This means that there is diffuse overall emission covering the whole nucleus, and more compact emission with narrower line widths, as in the case of Arp 220 (Lonsdale et al. 1998). The fact that even the nar-

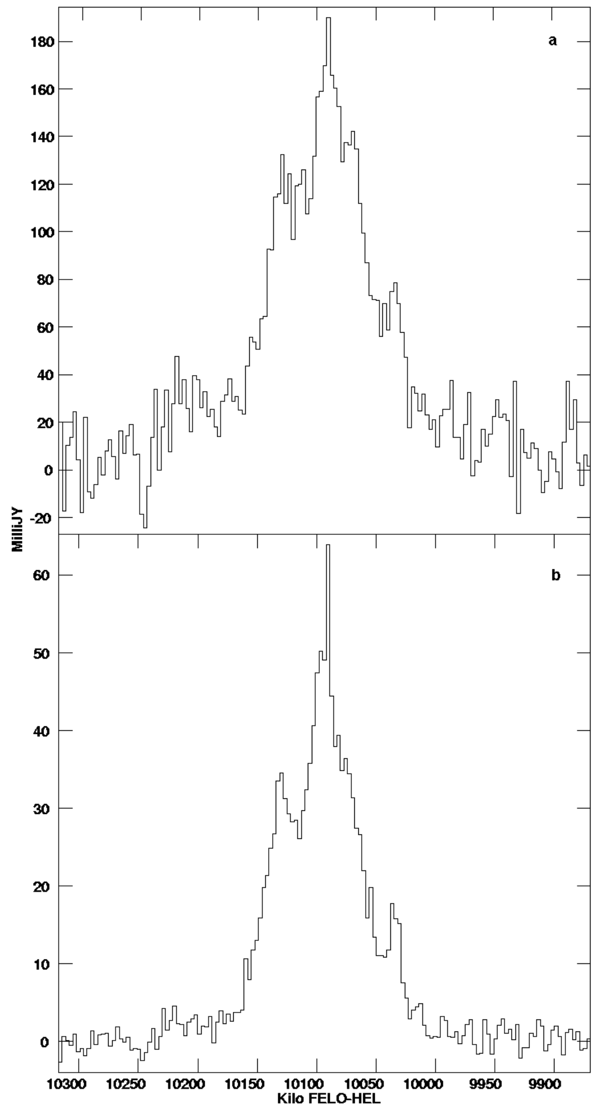

Fig. 5. The spectra of 10039. Spectrum (a) refers to the whole galaxy and spectrum (b) to a small region in the center of emission.

row line has a FWHM of ∼ 70 km/sec and clearly shows multiple components shows us that there are even more compact features which are unresolved. An Arp 220 like model, where we have maser emission of two kinds, compact and diffuse (Lonsdale et al. 1997) may well be the case for IRAS 10039-3338, and the broad underlying emission comes from an overall rotating disk containing the different emission regions. The geometry of the galaxy does not help us clearly distinguish between these regions, as they seem to be overlapping each other in the line of sight.

4. Conclusions

The 1.6 GHz continuum emission of Arp 220 has a double component structure; the two components are separated by ∼ 1 arcsec (=370 pc) and are at the same positions as the 1.4 GHz, the 4.8 GHz and the 1.3 mm continuum emission and HI emission and CO absorption. In the eastern region, the maser emission comes from the same place, in agreement with the early model by Baan (1985). There is also a velocity gradient in this region, suggesting that there is a rotating nuclear disk, the rotation however is not keplerian. In the western region the maser comes from areas north and south of the continuum, suggesting that it is unsaturated.

IRAS 10039-3338 looks like it consists of multiple components (three are detected). The overall spectrum has a very broad component, possibly coming from an overall rotating disk, and other very narrow components, pointing toward the existence of compact, parsec-sized emission regions, as in the archetypal Arp 220.

Acknowledgements. MERLIN is a national facility operated by the University of Manchester at Jodrell Bank Observatory on behalf of PPARC. The VLBA is an instrument of the National Radio Astronomy Observatory, a facility of the NSF operated under cooperative agreement by Associated Universities, Inc. E.R. would like to thank the Greek State Scholarships Foundation, without its financial support this work would not have been possible. E.R. and P.J.D. acknowledge partial support from the EC ICN RadioNET (Contract No. HPRI-CT-1999-40003).

References

Baan, W. A., Wood, P. A. D. & Hashick, A. D. 1982, ApJ, 260, L49
Baan, W. A. 1985, Nature, 315, 26
Baan, W. A. & Hashick, A. D. 1995, ApJ, 454, 745B
Carilli, C. L. & Taylor, G. B. 2000, ApJ, 532, L95
Diamond, P. J., Norris, R. P., Baan, W. A. & Booth, R. S. 1989, ApJ, 340, L49
Diamond, P. J., Lonsdale, C. J., Lonsdale, C. J., Smith, H. E. 1999, ApJ, 511, 178D
Kazès, I., Mirabel, I. F. & Combes, F. 1988, IAUC, 4629
Kazès, Proust, D., Mirabel, I. F., Combes, F., Balkowski, C. & Martin, J. M. 1990, A&A, 237, L1
Killeen, N. E. B., Staveley-Smith, L., Wilson, W. E. & Sault, R. J. 1996, MNRAS, 280, 1143
Lonsdale, C. J., Lonsdale, C. J., Diamond, P. J., Smith, H. E. 1998, ApJ, 493, L13
Mundell, C. G., Ferruit, P. & Pedlar, A. 2001, ApJ, 560, 168M
Philström, Y. M., Conway, J. E., Booth, R. S., Diamond, P. J. & Polatidis, A. G. 2001, A&A, 377, 413P
Sakamoto, K., Scoville, N. Z., Yun, M. S., Crosas, M., Genzel, R. & Tacconi, L. J. 1999, ApJ, 514, 68S
Sanders, D. B & Mirabel, I. F. 1996, ARA&A, 34, 749S
Smith, H. E., Lonsdale, C. J., Lonsdale, C. J., Diamond, P. J. 1998, ApJ, 493L, 17S
Yates, J. A., Richards, A. M. S., Wright, M. M., Collett, J. L., Gray, M. D., Field, D. & Cohen R. J. 2000, MNRAS, 317, 28Y